LIGHT REFLECTION MODEL OF PIXEL-BASED SURFACE PATCH FOR SHOT PEENING COVERAGE ESTIMATION

Xiao-Wei Tu, Claude Perron

Automation, Robotics and Intelligent Manufacturing Systems
Aerospace Manufacturing Technology Centre / Institute for Aerospace Research
National Research Council Canada
5145 Decelles Avenue, Montreal, QC, CANADA H3T 2B2

ABSTRACT
Nowadays, we need to efficiently control key parameters of the shot-peening process such as shot size, energy and peening angle, to ensure a positive and optimum effect on fatigue life. A good way to help us in adjustment of these parameters is to observe the resulting coverage after peening. Manual measurement and control of peening coverage – which consist of a visual inspection step by an operator – are highly subject to inspector interpretation, experience and error. Actually, however, they are still the main method of peening coverage estimation. An automatic visual inspection system was developed in this study to obtain stable evaluation data. We worked on a sequence of images of a peened surface illuminated with different lighting configurations. With the help of a ray reflection model, we implemented our algorithm for coverage estimation by shape from shading approach.

KEY WORDS Automatic surface inspection, Coverage estimation, Shot-peening, Context coherent constraints, Light reflection model

INTRODUCTION
In the last few decades, researchers and technicians have been increasingly attracted by the idea of automatic visual inspection of shot-peened surfaces for 2 reasons: 1. it is a primary step towards eventually automating the process with a robot guided by a machine vision system; and 2. it is a rapid research and development (R&D) tool for quality control such as coverage estimation, a unique and reliable method unlike traditional, manual, visual inspection that is subject to inspector error.

The main challenge in implementing such a system is the construction of a robust algorithm running on an inspection workstation, providing very reliable inspection results. In the present article, we describe such an algorithm developed in our laboratory for coverage estimation. Previously, we reported our research in this field with 2D texture analysis (Tu et al., 2007), which included a learning phase to estimate coverage by comparing known coverage samples. We obtained relative estimated results with reference to samples. Though very impressive data were generated, the method remains very relative in the sense that we need to present *a priori* known coverage samples to the system before targeting new pieces for estimation. We have been seeking an absolute way of modeling a peened surface directly, and our ultimate goal is to construct such an inspection system.

In the following sections, we describe a new coverage estimation method using shape from shading approach, including 3D surface characteristics. Mapping from a

3D surface structure to 2D coverage is undertaken by considering only projection of the indentation form to its button plan; material overflow forming annulets after impact is ignored. As coverage at this research point is not yet well-defined, annulets could be considered as part of the indentation form in shot peening. First, we will present our algorithm based on the reflection model as well as the hardware we deploy to cast shades by varying illumination angles in image sequence registration. Then, the test results will be reported to demonstrate the viability and robustness of the method. Finally, the study's conclusion will be drawn.

METHODS

For absolute surface coverage estimation after shot peening, we need to model the initial surface in 3D structure such as annulets and indentations. One of the methods for 3D recovery from 2D projection is shape from shading. Some very natural questions that arise here are: how do we distinguish if the pixels are cast by shade or not, and how do we determine the orientation of a surface patch affecting pixel brightness in the image? More than one image are often necessary to ascertain these characteristics by varying the illumination condition or viewing point during acquisition. In this study, a sequence of images is acquired with different illumination angles toward the inspection surface. Camera position relative to the surface is fixed; a pixel at the same position in image sequence with a different grey level represents the same surface patch shined and reflected differently. Images serve to infer the orientations of all patches represented by pixels. As the patches form the peened surface, we can know their 3D structures by their orientations. Previously, several image sequence processing approaches were reported for shot peening coverage estimation (Puente Leon, 2001), metal surface inspection (Puente Leon & Beyerer, 1997) and shot-peened surface inspection (Puente Leon, 2000), but they did not explore 3D structure and light modeling.

Hardware configuration

The system's hardware comprises a high-resolution camera with macro lens, a programmable LED ring light with certain modifications, a mechanical frame with height and angle adjustable for camera support and a Windows workstation for image analysis as well as control of the whole acquisition process. The workstation, ring light and its controller are shown in Figure 1a and 1b. We made a minor modification to obtain 8 point light sources. Connection via a serial port between the ring light controller and the workstation allows us to sequentially synchronize image acquisition by switching the LED on and off in an angular direction. The images are transferred to the workstation through an IEE1394 cable.

Algorithm

We consider that each image pixel corresponds to a small patch of the whole peened surface. Magnification of the surface detail can be adjusted such that each patch projected to image with at least the size of a pixel should be roughly planar with a unique normal, so that resolution of the CCD inside the camera delimits the surface area to be inspected. Neighbouring patches form a portion of the spherical crater that corresponds to an indentation on the peened surface. For shot peening coverage estimation, we need to classify each image pixel into 2 categories: a pixel from a peened or an intact patch. The ratio of total pixels in these 2 categories gives us correct coverage estimation. The classification algorithm is based on applying 3

context-coherent constraints to the normal direction of the patch that each pixel represents compared to its neighbours. With a pixel from a peened patch: 1. its normal should not be vertical to the entire surface or parallel to the camera optical axis except for those patches forming the deep bottom of a crater; 2. all normal lines of neighbouring patches intersect at a common virtual point above the surface which is the centre of the spherical crater; the distance between the centre and any patches inside the crater should be equal to approximately the radius of indentation. This distance helps to recover pixels rejected by the first constraint and to re-class them from an intact to a peened pixel; 3. the change in normal direction of all neighbouring patches should be gradual, not only circular along its tangential direction inside the spherical form at different depths, but also in its radial direction among different depths; any abrupt or random variation in normal direction invalidates related pixels as peened pixels. As we can see so far, a reliable estimation of the normal direction of all patches from their corresponding pixels in image is a key step, whereas classification is trivial. Generally, theoretical considerations in light reflection can be expressed as: *Light incident at a surface = Light reflected + Light scattered + Light absorbed + Light transmitted.*

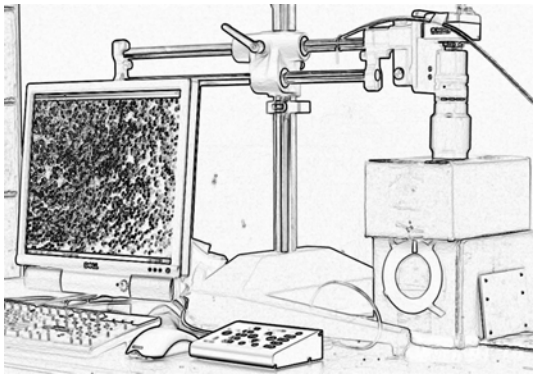

Fig.1a. Image acquisition station

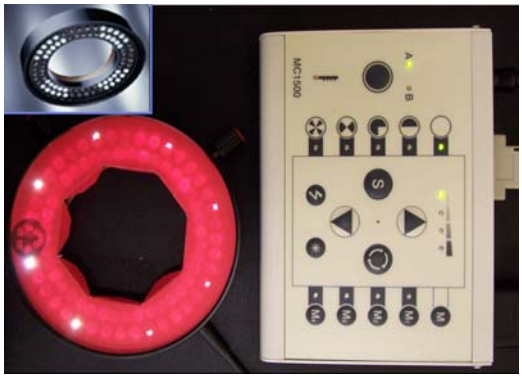

Fig. 1b. Ring light and its controller

As we consider an opaque, typically non-absorbed surface, light captured by the CCD sensor at a particular point (pixel) can be simplified as formula (1):

$$I_c = I_a k_a + I_i (k_d (\mathbf{L} \cdot \mathbf{N}) + k_s (\mathbf{R} \cdot \mathbf{V})^n) \qquad (1)$$

where I_c is the light captured by the CCD, I_a is the ambient component, I_i is the incident light, k_a, k_d and k_s are the contributing weights of ambient, diffuse and specular components, $\mathbf{L}$, $\mathbf{N}$, $\mathbf{R}$ and $\mathbf{V}$ are unit vectors indicating the direction of incident light, normal of the reflecting surface, reflecting light direction and viewer's observation direction, *n* is an index simulating surface roughness; for a perfect mirror, *n* would be infinity, and reflected light would be constrained to the mirror reflection direction, with almost no specular component at all elsewhere. In Figure 2, we show all mentioned vectors and the model called the Phong reflection model (Phong, 1975), which is largely used in image synthesis and ray-tracing applications.

If we apply a 2D imaging system to this work, the normal direction estimation algorithm of a small patch on a surface is mainly based on a simplified Phong light reflection model. There are 3 terms in the reflection model (1) which correspond to: ambient, diffuse and specular light components on a surface. The sum of the contribution of these terms is what a viewer or a camera can see or capture: the light intensity at a particular point of the surface. The ambient term in (1) can be ignored in

a closed and controlled lighting environment, and a minor modification of the model is that *n* tends to be very great as we are dealing with an aluminium metal surface; also, we can always include the roughness index inside k_s; the term $k_s(\mathbf{R}\bullet\mathbf{V})^n$ tends to be infinitely small, so the grey level of a pixel in image is the total contribution of diffuse light on that patch, which is a linear function of the normal direction of that patch except when $\mathbf{R}$ and $\mathbf{V}$ are collinear, and the specular component, whose value tends to k_s of (1), becomes dominant.

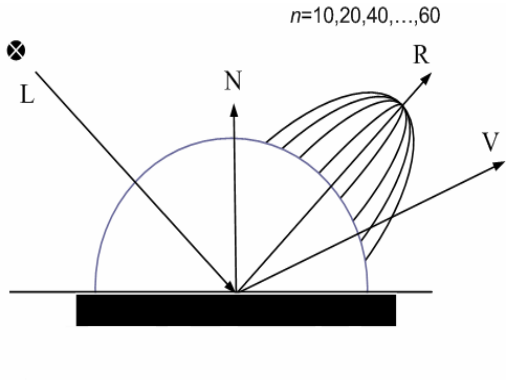

Fig. 2. Phong reflection model

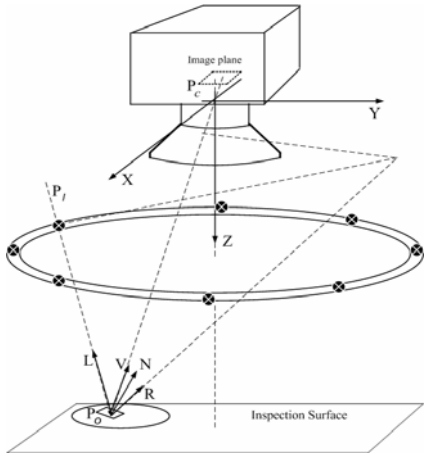

Fig. 3. Physical configuration

The following is our implementation of a normal direction estimation algorithm: refer to Figure 3 for the physical configuration and the coordinate system established in our optical set-up. The normal of each patch can be expressed as an unknown $\mathbf{N}:(n_1,n_2,n_3)$ unity vector of 3 components. The small patch at position $\mathbf{P}_o:(x_o,y_o,z_o)$ can be modeled as a plane whose equation is: $\mathbf{N}\cdot(\mathbf{P}-\mathbf{P}_o)=0$. It is impossible to recover this vector merely from the grey level intensity of a pixel in 1 snapshot. With the programmable LED ring light, LED segments can be switched on and off timely, which allows us to acquire several images in different lighting angles (say 8 images in a sequence) without any change of physical hardware setting. For each pixel, we get a vector of 8 grey levels $\mathbf{G}_c:(g_{c1},g_{c2},...,g_{c8})$. Incident light angles can be computed by a normalized vector with light source positions $\mathbf{P}_l:(p_{l1},p_{l2},p_{l3},...,p_{l8})$ and patch position $\mathbf{P}_o$, namely:

$$\mathbf{L}=\frac{(\mathbf{P}_l-\mathbf{P}_O)}{\sqrt{(\mathbf{P}_l-\mathbf{P}_O)\cdot(\mathbf{P}_l-\mathbf{P}_O)^T}} \qquad (2)$$

in the original Phong model. $\mathbf{V}$ can be computed as:

$$\mathbf{V}=\frac{(\mathbf{P}_C-\mathbf{P}_O)}{\sqrt{(\mathbf{P}_C-\mathbf{P}_O)\cdot(\mathbf{P}_C-\mathbf{P}_O)^T}} \qquad (3)$$

if the camera is at position $\mathbf{P}_c:(x_c,y_c,z_c)$. We claimed previously that the grey level of a pixel reflected by a small patch on a surface is a linear function of normal direction of that patch since the contribution of the specular component is very small and can be ignored in most cases when $\mathbf{R}$ and $\mathbf{V}$ are not collinear. However, vector $\mathbf{R}$, still a function of $\mathbf{N}$, can be computed as $\mathbf{R}=\mathbf{L}+2*\mathbf{N}*(\mathbf{L}\cdot\mathbf{N})$ (refer to Figure 4), which is obviously not a linear function of $\mathbf{N}$. Fortunately, we do not need to consider it

further as its contribution to the final grey level is very small as $\lim_{n\to\infty}(\mathbf{R}\cdot\mathbf{V})^n \to 0$. In fact, when the specular component is dominant, $\mathbf{N}$ can be computed directly from $\mathbf{L}$ and $\mathbf{V}$ ($\mathbf{R}$) as $\mathbf{N} = Norm(\frac{1}{2}(\mathbf{R}-\mathbf{L}))$ or $\mathbf{N} = Norm(\frac{1}{2}(\mathbf{V}-\mathbf{L}))$ as $\mathbf{R} = \mathbf{V}$: refer to Figure 4 for these vector computations. Experimental results have shown that when the grey level of a pixel is saturated at a certain configuration, using it for $\mathbf{N}$ recovery is not robust. The specular component gives us only a hint to directly apply vector computation for $\mathbf{N}$, but the decision that a pixel is saturated or not is very error-prone, much like a brutal thresholding operation, and also since the dynamic range of a CCD is quite limited in most situations. We always prefer a set of linear equations to estimate $\mathbf{N}$.

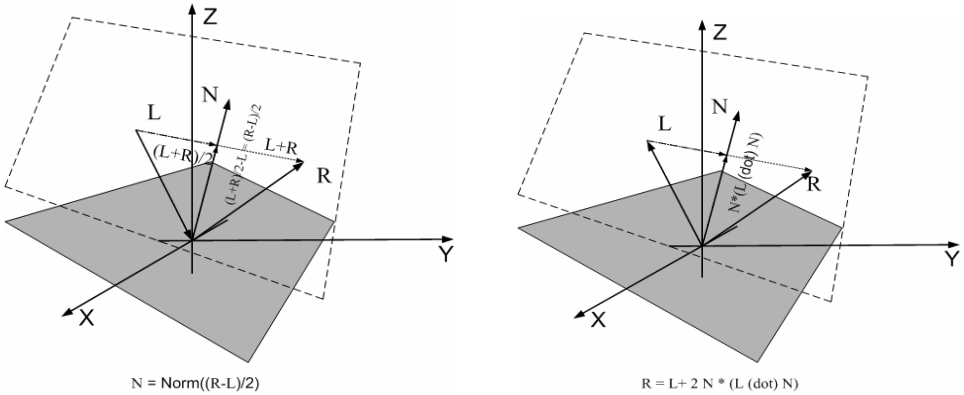

Fig. 4. Vector computation

From a different incident light angle towards a patch as input, and grey levels of the same pixel in images as output, we can establish over-determined linear equation sets to solve the unknown vector $\mathbf{N}$ of that patch. The Phong reflection model (1), without the specular component as a linear function of $\mathbf{N}$, can be expressed as (4):

$$\mathbf{G}_c^T = \mathbf{K}_{8\times3} \bullet \mathbf{N}^T \qquad (4)$$

where for a given patch at position $\mathbf{P}_o$, with constant intensity of incident light and its position $\mathbf{P}_l$, the constant matrix $\mathbf{K}_{8\times3}$ is totally dependent on I_i and k_d constants as well as on $\mathbf{L}$ and $\mathbf{V}$ vectors – see (2) and (3) − which are also constant when $\mathbf{P}_o$, $\mathbf{P}_l$ and $\mathbf{P}_c$ are given. A good normal direction of patch can be estimated by the least mean squares solution of $\mathbf{N}$ for (4):

$$\mathbf{N} = (\mathbf{K}_{8\times3}^T \bullet \mathbf{K}_{8\times3})^{-1} \bullet \mathbf{K}_{8\times3}^T \bullet \mathbf{G}_c^T \qquad (5)$$

The same procedure can be applied to the entire surface image under observation, and we get a resulting image of normal vectors from solution (5). By applying the context coherent constraints mentioned at the beginning of this section to the image, we classify all pixels into 2 desired categories: pixels from an indentation or from a non-impact surface. A simple counting post-process is employed to obtain a coverage estimation result.

The experimental data reveal that our method is very robust in the sense that the percentage of coverage estimated with the system is repeatable with a well-adjusted

hardware setting. Even the lighting position, physical configuration and lens focus are not perfectly set; the result of coverage estimation is still converged to the correct answer.

RESULTS

In this section, we show the outcome of the above algorithm. A set of known coverage of peened aluminium samples was provided by one of our clients, and a sequence of 8 images per sample was taken by our system with 8 different positions of LED switched on and off by timer. Time for acquiring an image sequence is about 400 mille-seconds. The physical viewing field is 24 mm X 24 mm for an image of 640 by 480 pixels, and indentation size is less than 0.8 mm. The processing time from normal vector image computation to pixel classification takes roughly 800 mille-seconds on a Pentium IV workstation. The total coverage estimation result with our algorithm is very close to the known coverage (data provided only by our client). An example is presented in Figure 5 with peened coverage of 50%. Because of publication space limitations, we present only 1 image at position 6 in the 8-image sequence. The original image was taken with diffused lighting which displayed a clear view of the sample surface. The final classification was a binary image in which white areas represented the grouping of indentation parts, and the black areas were non-impact surface parts. The ratio between the number of white pixels and total image pixels was 0.5002 in this case.

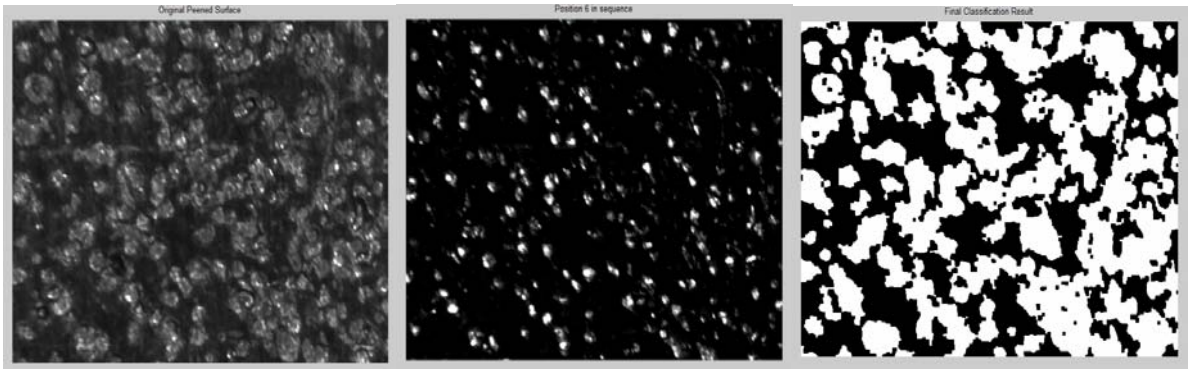

Fig. 5. Original image 6th image in sequence Final classification result

CONCLUSION

We have carefully examined the normal vector image computed on the basis of shape from shading algorithm. Globally, the vectors represent well the normal direction of patches on the physical surface. The more images with different lighting positions we obtain in image sequence, the more reliable are the normal vectors computed. Smoothness in normal direction within neighbouring pixels is not always preserved because of initial surface roughness, the inherent pattern left during manufacturing of the surface and multiple overlapping indentations. This means that in certain parts of the image, it is difficult to apply context coherent constraint. Overlap occurs more frequently as exposure to shot time lasts. The recovery of pixels rejected by the first constraint, in the case of a normal vector that is parallel to the camera's optical axis by radius distance constraint, is not stable as expected owing to the error in position computation of the common normal intersection point, which explains why we can see dark, small holes inside white grouped pixels in the final classification result panel of Figure 5. It appears that the denser is the coverage, the tougher is the recovery of bottom patches in the craters. Fortunately, the number of

these pixels is usually minor, which does not affect a lot of total coverage estimation results.

REFERENCES

Tu X, Larose S and Perron C. Determination of shot peening coverage using the texture analysis approach. Aerospace Manufacturing & Automated Fastening Conference, September 17-20, 2007, Los Angeles, California, USA.

Puente Leon F. Determination of the coverage of shot peened surfaces. Surface Treatment, June 20-22, 2001, Seville, Spain. WIT Press, Southampton.

Puente Leon F and Beyerer J. Active vision and sensor fusion for inspection of metallic surfaces. Intelligent Systems & Advanced Manufacturing, Pittsburgh, Pennsylvania, USA, October 13-17, 1997, Proc. SPIE.

Puente Leon F. Model-based inspection of shot peened surfaces using fusion techniques. Intelligent Systems for Advanced Manufacturing, Boston, Massachusetts, USA, November 5-8, 2000, Proc. SPIE.

Phong B. Illumination for computer-generated pictures. Comm ACM 1975;18(6):311-17.